

# Which is the Strongest Peak among 104, 113 & 116-Reflections of Corundum ?

Takashi Ida  
Advanced Ceramics Research Center,  
Nagoya Institute of Technology, Japan  
[ida.takashi@nitech.ac.jp](mailto:ida.takashi@nitech.ac.jp)



## Introduction

ICDD PDF-4+ 2023 lists 23 star-quality data sets of corundum ( $\alpha$ -Al<sub>2</sub>O<sub>3</sub>), where 21 sets (00-046-1212, 01-070-5679, 01-070-7364, 01-071-1683, 01-075-1862, 01-075-1863, 01-075-6775, 01-082-1399, 01-088-0286, 01-089-7715, 04-004-2852, 04-004-5434, 04-005-4213, 04-005-4505, 04-007-1400, 04-007-4873, 04-015-8608, 04-015-8993, 04-015-8994, 04-015-8995 & 04-015-8996) assign the strongest peak to 104-reflection, and 2 sets (01-089-7716 & 01-089-7717) assign the strongest peak to 113-reflection.

NIST certifies 113-reflection is the strongest, 116-reflection is the 2<sup>nd</sup> strongest, and 104-reflection is the 3<sup>rd</sup> strongest for SRM676a standard  $\alpha$ -Al<sub>2</sub>O<sub>3</sub> powder, while 104-reflection is the strongest, 116-reflection is the 2<sup>nd</sup> strongest, and 1.0.10/119-reflections are the 3<sup>rd</sup> strongest for standard  $\alpha$ -Al<sub>2</sub>O<sub>3</sub> sintered disk SRM1976c.

Hubbard et al. (1976) have shown that it is expected that 116-reflection should be the strongest, 113-reflection the 2<sup>nd</sup> strongest, and 104-reflection the 3<sup>rd</sup> strongest for a neutral atom model Al<sub>2</sub><sup>0</sup>O<sub>3</sub><sup>0</sup>, while 113-reflection should be the strongest, 116-reflection the 2<sup>nd</sup> strongest, and 104-reflection the 3<sup>rd</sup> strongest for a fully-ionized model Al<sub>2</sub><sup>3+</sup>O<sub>3</sub><sup>2-</sup>.

## Crystallographic Data of Corundum

Trigonal,  $R\bar{3}c$  (No. 167),  $a = 4.759 \text{ \AA}$ ,  $c = 12.993 \text{ \AA}$  (hexagonal setting)

$c/a = 2.73$  ( $\alpha$ -Al<sub>2</sub>O<sub>3</sub>)  $\gg \sqrt{6} \approx 2.45$  (ideal hcp arrangement of oxygen)

$B_{\text{iso}} \equiv 8\pi^2 U_{\text{iso}} \approx 0.22 \text{ \AA}^2 \Leftrightarrow U_{\text{iso}} = 0.0028 \text{ \AA}^2$

TABLE I. Atomic positions and mean square displacements of  $\alpha$ -Al<sub>2</sub>O<sub>3</sub> from 5 data sets for 2 single crystals (Maslen et al., 1993)

	Crystal 1			Crystal 2	
	Data (1)	Data (2)	Data (3)	Data (4)	Data (5)
$z$ (Al)	0.352 2	0.352 2	0.352 2	0.352 2	0.352 2
$x$ (O)	0.694 2	0.693 8	0.693 8	0.694 0	0.694 0
$U_{11}$ (Al) ( $\text{\AA}^2$ )	0.002 4	0.002 1	0.002 5	0.002 5	0.002 5
$U_{33}$ (Al) ( $\text{\AA}^2$ )	0.002 7	0.002 5	0.002 4	0.002 4	0.002 4
$U_{11}$ (O) ( $\text{\AA}^2$ )	0.002 8	0.002 5	0.002 8	0.002 8	0.002 8
$U_{22}$ (O) ( $\text{\AA}^2$ )	0.002 7	0.002 6	0.003 0	0.003 0	0.003 0
$U_{33}$ (O) ( $\text{\AA}^2$ )	0.002 7	0.002 8	0.002 8	0.002 8	0.002 8
$U_{12}$ (O) ( $\text{\AA}^2$ )	0.000 3	0.000 3	0.000 3	0.000 3	0.000 3

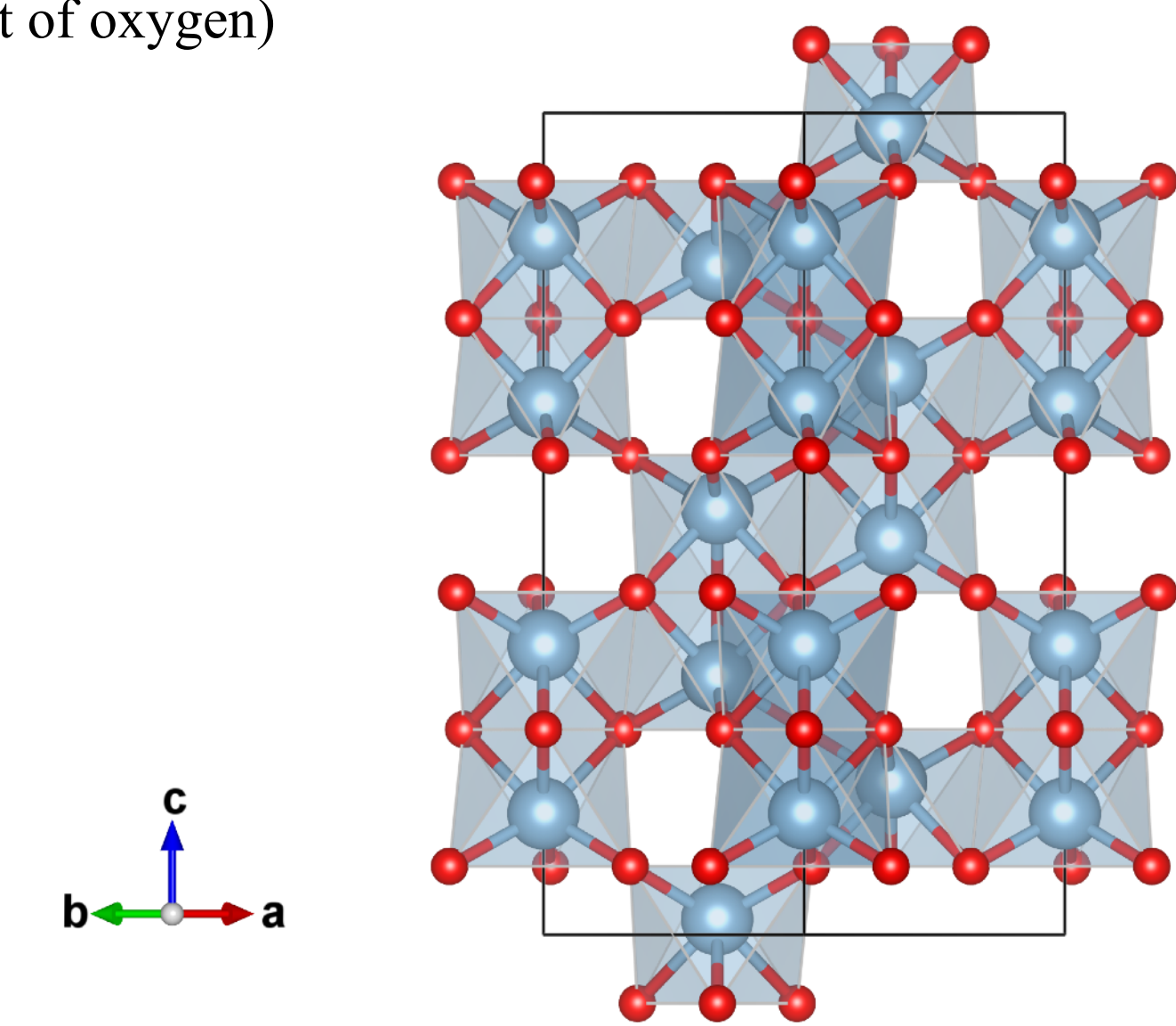


Figure 1. Projection of  $\alpha$ -Al<sub>2</sub>O<sub>3</sub> structure along [110]-direction in hexagonal setting, drawn with *VESTA* 3 (Momma & Izumi, 2011)

## Density Functional Theory (DFT) Calculation

*Quantum ESPRESSO 7.1* (Gianozzi et al., 2009, 2017) (open-source, free)

Pseudo-potential: projector-augmented wave (PAW) (Kresse & Joubert, 1999)

Exchange-correlation: local density approximation (LDA) (Perdew & Zunger, 1981) & Perdew-Burke-Ernzerhof (PBE) model (Perdew et al., 1996, 1997)

Electron density:  $60 \times 60 \times 60$ -mesh for rhombohedral (reduced) cell ( $a = 5.129 \text{ \AA}$ ,  $\alpha = 55.29^\circ$ )

↓ (Fourier transform + Dispersion correction)  $\times$  (Common atomic displacement)

↓ (Square absolute, Geometrical correction, Sum of equivalent reflections)

XRD peak intensities,  $I_{hkl}$

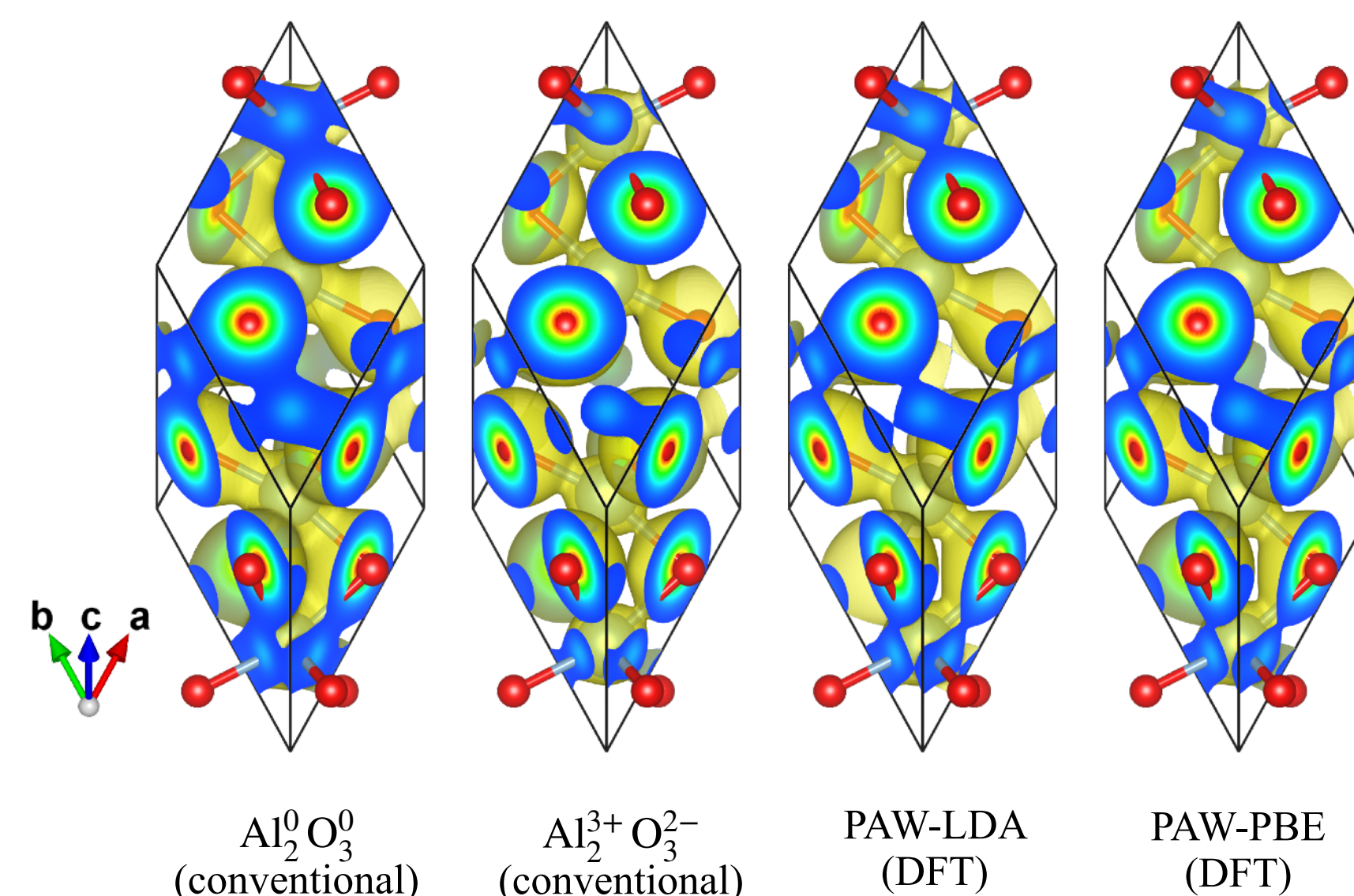


Figure 2. Projection of electron density iso-surface (yellowish color) at the level of  $0.3 \text{ e/\AA}^3$  along [112]-direction in rhombohedral setting, and color-scaled density map (red: high, blue: low) on the faces of the rhombohedral cell, rendered from  $60 \times 60 \times 60$  voxel data with *VESTA* 3 (Momma & Izumi, 2011)

## Experimental & Treatment of XRD Data

Powder #1 (High Purity Chemicals, 99.99%, 2–3  $\mu\text{m}$ )

Powder #2 (High Purity Chemicals, 99.99+%, ca 0.3  $\mu\text{m}$ )

Instrument: Rigaku MiniFlex (Cu  $K\alpha$ ) with silicon-strip X-ray detector

Deconvolutional Treatment (DCT) (Ida, 2021a)

Individual peak profile fitting with a symmetric profile function (Ida, 2021b)

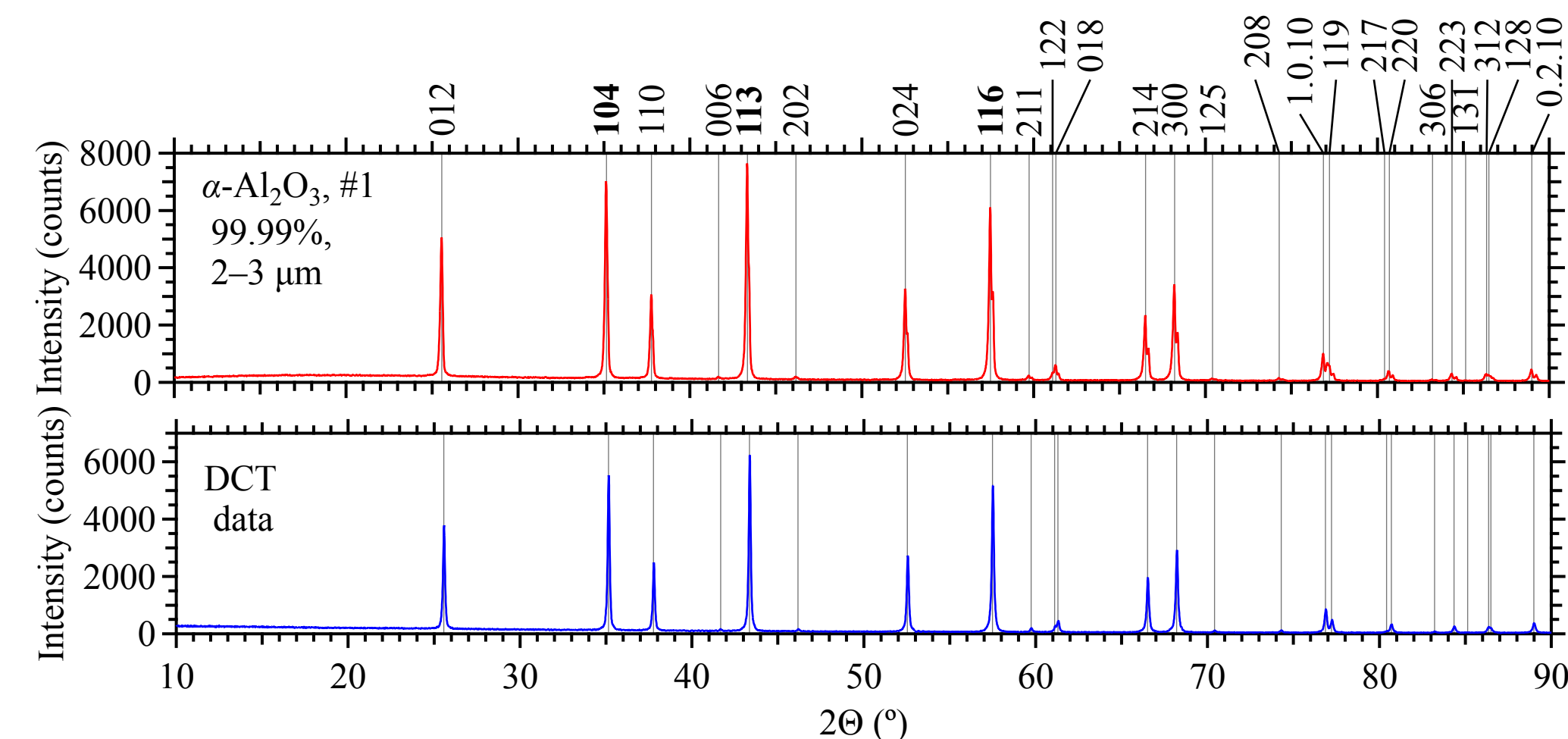


Figure 3. Observed (upper; red) and deconvolutionally treated (DCT) (lower; blue) X-ray diffraction intensity of  $\alpha$ -Al<sub>2</sub>O<sub>3</sub>. Vertical lines indicate the peak locations listed in PDF 00-046-1212.

Figure 4. Demonstration of DCT and automatic individual peak profile fitting with a symmetric function for 113-reflection of  $\alpha$ -Al<sub>2</sub>O<sub>3</sub>;  $w$ : HWHM of Lorentzian component,  $\sigma$  &  $k$ : standard deviation & excess kurtosis of symmetrized instrumental function.

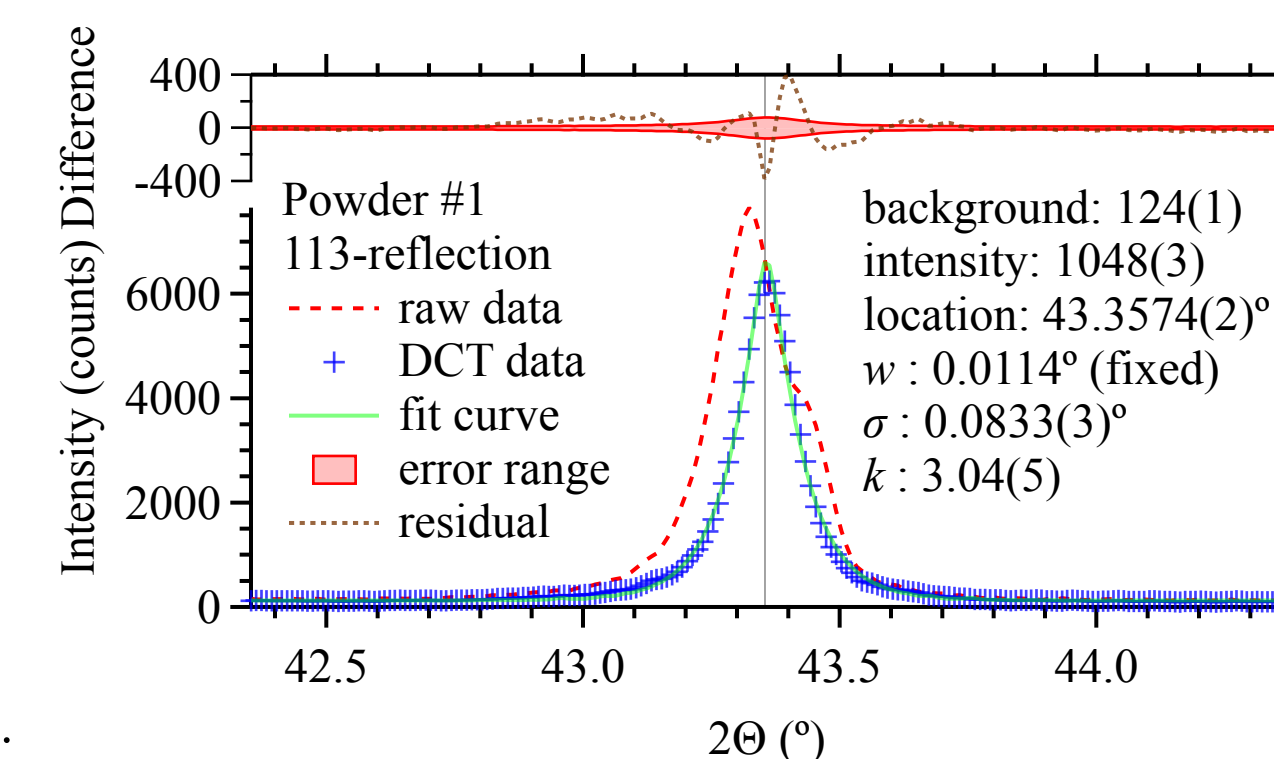


TABLE II. XRD relative intensities listed in ICDD PDF-4+, intensities certified for NIST SRM676a & SRM1976c, intensities for Al<sub>2</sub><sup>0</sup>O<sub>3</sub><sup>0</sup>, Al<sub>2</sub><sup>1.5+</sup>O<sub>3</sub><sup>-</sup> & Al<sub>2</sub><sup>3+</sup>O<sub>3</sub><sup>2-</sup> calculated by a conventional method, intensities calculated by DFT (PAW-LDA & PAW-PBE) methods, and intensities extracted from experimental data. Values in parentheses are differences from NIST SRM676a data.

$hkl$	ICDD PDF-4+		NIST		Conventional			DFT		Experimental	
	00-046-1212	01-089-7716	SRM 676a	SRM 1976c	Al <sub>2</sub> <sup>0</sup> O <sub>3</sub> <sup>0</sup>	Al <sub>2</sub> <sup>1.5+</sup> O <sub>3</sub> <sup>-</sup>	Al <sub>2</sub> <sup>3+</sup> O <sub>3</sub> <sup>2-</sup>	PAW LDA	PAW PBE	99.99% 2–3 $\mu\text{m}$	99.99+% ca 0.3 $\mu\text{m}$
	<div style="display: flex; justify-content: space-around; font-size: small;"> <span style="background-color: yellow; padding: 2px;">Strongest</span> <span style="background-color: #cccccc; padding: 2px;">2<sup>nd</sup> Strongest</span> <span style="background-color: #ffffcc; padding: 2px;">3<sup>rd</sup> Strongest</span> </div>										
012	45 (–12)	65.7 (+8.6)	57.1	24 (–33)	61.0 (+3.9)	59.3 (+2.2)	57.1 (+0.0)	54.1 (–3.0)	57.3 (+0.2)	56.8 (–0.3)	56.7 (–0.4)
104	100 (+12)	99.5 (+11.1)	88.4	100 (+12)	97.5 (+9.1)	94.5 (+6.1)	90.8 (+2.4)	79.8 (–8.6)	84.3 (–4.1)	87.3 (–1.1)	90.0 (+1.6)
110	21 (–17)	46.4 (+8.6)	37.8		45.6 (+7.8)	43.3 (+5.5)	40.8 (+3.0)	32.5 (–5.3)	34.0 (–3.8)	37.2 (–0.6)	36.0 (–1.8)
113	66 (–34)	100	100	37 (–63)	98.0 (–2.0)	99.4 (–0.6)	100	100	100	100	100
024	34 (–13)	48.0 (+0.7)	47.3	21 (–26)	50.5 (+3.2)	50.8 (+3.5)	50.7 (+3.4)	43.0 (–4.3)	42.7 (–4.6)	46.3 (–1.0)	45.7 (–1.6)
116	89 (–7)	94.2 (–1.6)	95.8	88 (–8)	100 (+4.2)	100 (+4.2)	99.3 (+3.5)	86.7 (–9.1)	88.2 (–7.6)	92.6 (–3.2)	95.2 (–0.6)
214	23 (–15)	35.1 (–2.6)	37.7		40.5 (+2.8)	40.6 (+2.9)	40.5 (+2.8)	33.3 (–4.4)	33.1 (–4.6)	36.1 (–1.6)	34.9 (–2.8)
300	27 (–31)	54.1 (–3.4)	57.5	12 (–46)	61.9 (+4.4)	61.5 (+4.0)	60.6 (+3.1)	53.0 (–4.5)	52.7 (–4.8)	56.4 (–1.1)	52.3 (–5.2)
$\delta_{\text{RMS}}$	20%	6.0%		37%	5.2%	3.9%	2.6%	5.6%	4.4%	1.4%	2.3%

$\delta_{\text{RMS}}$ : Root mean square difference from NIST SRM676a intensities